Journal of Molecular Structure 1180 (2019) 491–498

Contents lists available at ScienceDirect

Journal of Molecular Structure

journal homepage: http://www.elsevier.com/locate/molstruc

# Calcium complexing behaviour of lactate in neutral to highly alkaline medium

Csilla Dudás [a], Bence Kutus [a], Éva Bószörményi [a], Gábor Peintler [a], Amr A.A. Attia [b], Alexandru Lupan [b], Zoltán Kele [c], Pál Sipos [a], István Pálinkó [a, *]

[a] Material and Solution Structure Research Group, Institute of Chemistry, University of Szeged, H–6720 Szeged, Hungary
[b] Department of Chemistry, Babeş-Bolyai University, RO–400028 Cluj-Napoca, Romania
[c] Department of Medical Chemistry, University of Szeged, H-6720 Szeged, Hungary

ARTICLE INFO

*Article history:*
Received 30 October 2018
Received in revised form
29 November 2018
Accepted 5 December 2018
Available online 7 December 2018

*Keywords:*
Ca complexing properties of D,L lactate
Neutral and alkaline medium
NMR spectroscopy
ESI-MS spectroscopy
Molecular modelling

ABSTRACT

The calcium complexing properties as well as the acid-base behaviour of D,L-lactate have been investigated in both neutral and alkaline media by Ca-ISE potentiometry, $^{13}C$ NMR spectroscopy, ESI-MS spectroscopy and solubility measurements. In close to neutral solutions the formation of the $CaLac^+$ and $CaLac_2^0$ complexes were detected with formation constants of $\log K_{1,1} = 0.99 \pm 0.02$ and $\log \beta_{1,2} = 1.42 \pm 0.03$ ($I = 4$ M, $T = 25$ °C). These data are consistent with previously reported literature data measured at lower ionic strengths. The alkaline deprotonation constant of lactate has been determined to be $pK_a = 15.8 \pm 0.2$. In highly alkaline medium, the formation of the $CaLacOH^0$ and $CaLac(OH)_2^-$ complexes were detected with the corresponding formation constants being $\log \beta_{1,1,1} = 1.35 \pm 0.09$ and $\log \beta_{1,1,2} = 1.43 \pm 0.06$. The structures of the $CaLac^+$ and $CaLacOH^0$ complexes were optimized by molecular modelling calculations.



## 1. Introduction

Hydroxy carboxylates are known to be effective complexing agents. In neutral medium, both the carboxylate and the hydroxy groups are possible binding sites. Their complexing ability, however, is more pronounced in alkaline medium, where the hydroxy groups may be deprotonated yielding a more efficiently sequestering alcoholate function.

Under the highly saline and highly alkaline conditions prevailing in low and intermediate level (L/IL) radioactive waste repositories, the presence of small molecular metal chelators are considered to have significant impact on the mobilization of actinides and lanthanides [1–5]. Such complexing agents are formed during the alkaline degradation of cellulose, which is present in these L/IL wastes in significant quantities [6–9]. The main degradation product of cellulose is α-D-isosaccharinate; however, lactate (2-hydroxypropanoate, $Lac^-$) was also shown to be formed in the course of these reactions [6,10–12].

The complex formation of $Lac^-$ has been studied with a series of metal ions [13]. In neutral solutions containing both $Ca^{2+}$ and $Lac^-$ ions, the formation of the plausible $CaLac^+$ complex was detected. The formation constant, $\log K_{1,1}$, was found to be 0.48–1.47 at 25 °C at the ionic strength ($I$) range of 0–1 M [13–21]. In some of these works, however, the formation of the neutral $CaLac_2^0$ complex was also reported [20,21]. The corresponding stability products, $\log K_{1,1}$ and $\log \beta_{1,2}$, were determined to be 0.90 and 1.24 [20] as well as 0.92 and 1.62 [21]. The binding sites of $Lac^-$ in the $CaLac^+$ complex were also revealed by $^{13}C$ NMR spectroscopic measurements. $Lac^-$ was found to act as a bidentate ligand binding $Ca^{2+}$ through both the $COO^-$ and the OH groups [22]. For the $MgLac^+$ species, conversely, the ligand was suggested to be bound to the $COO^-$ moiety through a water molecule forming a solvent-shared ion-pair [22].

In acidic medium, in the presence of lanthanides, the formation of $MLac^{2+}$, $MLac_2^+$, $MLac_3^0$ and $MLac_4^-$ has been shown, where M = La(III), Ce(III), Pr(III), Nd(III), Sm(III), Eu(III), Gd(III), Tb(III), Dy(III), Ho(III), Er(III), Tm(III), Yb(III) and Lu(III) [23]. The coordination environment of the La(III)-lactate complexes was studied by DFT calculations [24]. Barkleit et al. also suggested the formation of $AmLac^{2+}$, $AmLac_2^+$ and $AmLac_3^0$ as well as $EuLac^{2+}$, $EuLac_2^+$ and $EuLac_3^0$ in the presence of Am(III) and Eu(III), respectively [25]. In Nd(III)-containing solutions, the presence of $NdLac^{2+}$, $NdLac_2^+$ and

* Corresponding author.
*E-mail address:* palinko@chem.u-szeged.hu (I. Pálinkó).

https://doi.org/10.1016/j.molstruc.2018.12.020
0022-2860/

$NdLac_3^0$ has been proposed [26].

To the best of our knowledge, the behaviour of $Lac^-$ in highly alkaline medium has not been investigated before. The scope of the present work was to describe the composition, stability and structure of complexes forming between $Lac^-$ and $Ca^{2+}$ both in neutral and highly alkaline media at high ionic strength ($I = 4.0$ M) relevant to nuclear waste disposal.

## 2. Experimental

### 2.1. Reagents and solutions

$CaCl_2$ stock solutions were prepared by dissolving $CaCl_2 \cdot 2H_2O$ (Sigma Aldrich, $\geq$ 99% purity) in water. The exact concentrations of the solutions were determined by complexometric titrations using EDTA. Stock solutions of NaOH were made by diluting a carbonate-free concentrated NaOH solution [27], and were standardized against HCl of known concentration. Sodium lactate solutions were prepared by neutralizing racemic D,L-lactic acid (Acros Organics, 85% m/m) with NaOH. The ionic strength was adjusted to 4.0 M by sodium chloride (Molar Chemicals, a. r. grade) in each sample. Milli-Q Millipore water was used to prepare all solutions.

### 2.2. Potentiometric titrations

Potentiometric titrations were performed with the aid of a Metrohm 794 Titrando instrument using a combined calcium ion selective electrode (Ca-ISE) from Metrohm. All measurements were carried out at constant 4.0 M ionic strength in a double-jacketed titration cell thermostated to $(25.0 \pm 0.1)$ °C, and the titrands were stirred continuously during the reactions.

For the calibration of the electrode, a solution containing $[Ca^{2+}]_{T,0} = 10^{-4}$ M with $V_0 = 45$ mL initial volume was titrated with 0.2030 M $CaCl_2$ up to $V = 95$ mL. Hereafter, for species X, $[X]_{T,0}$ or $[X]_T$ denotes its initial total concentration (titrations) or total concentration (NMR and solubility measurements), while [X] represents its equilibrium concentration. The response of the Ca-ISE was determined in the $-4.0 < \log([Ca^{2+}]/M) < -1.5$ range, and was found to deviate from the Nernstian (linear) behaviour at the two ends of this interval. Thus a nonlinear calibration procedure was used by fitting splines into the calibration curve using the Spline Calculus program [28]. Three sets of measurements were performed with solutions containing $[Ca^{2+}]_{T,0} = 10^{-4}$ M and $[Lac^-]_{T,0} = 0.105$, 0.240, 0.480 M using the same titrant as for the calibration.

### 2.3. $^{13}C$ NMR measurements

$^{13}C$ NMR spectra were recorded on a Bruker Avance DRX 500 MHz spectrometer equipped with a 5 mm inverse broadband probe head furnished with *z*-oriented magnetic field gradient capability. The magnetic field was stabilized by locking it to the $^2D$ signal of the solvent prior to the measurements. The sample temperature was set to $(25 \pm 1)$ °C during all spectra acquisitions. For the individual samples, 128 or 256 scans were collected to record the $^{13}C$ NMR spectra. Each highly alkaline solution was placed into a PTFE liner, and the liner was placed into an external quartz tube containing $D_2O$.

To study the behaviour of $Lac^-$ in the presence of $Ca^{2+}$ in (close to) neutral medium, a solution set containing $[Lac^-]_T = 0.321$ M and $[Ca^{2+}]_T = 0$–1.029 M was prepared. To determine the deprotonation constant of the hydroxy group of $Lac^-$, two solution sets were prepared with $[Lac^-]_T = 0.0960$ and 0.1525 M, while $[OH^-]_T$ was systematically increased from 0 to 3.871 and 2.630 M, respectively.

### 2.4. ESI-MS measurements

ESI-MS measurements were performed in positive ion mode using a Micromass Q-TOF Premier (Waters MS Technologies, Manchester, UK) mass spectrometer equipped with an electrospray ion source. Samples were introduced into the MS by using the direct injection method: the built-in syringe pump of the instrument with a Hamilton syringe was used. The electrospray needle was adjusted to 3 kV, and $N_2$ was used as the nebulizer gas.

For ESI-MS experiments, a solution was prepared by dissolving CaO in a solution of lactic acid in order to exclude the presence of sodium ions. The thus obtained solution contained $[Lac^-]_T = 0.10$ M and $[Ca^{2+}]_T = 0.05$ M.

### 2.5. Solubility measurements supplemented with ICP-OES

In order to determine the formation constant of the complex(es) forming in highly alkaline medium, a solution set was prepared as follows: solutions containing $[Lac^-]_T = 0.5$ M and $c_{NaOH} = 0.14$–2.64 M were prepared. After that, 0.2 g solid CaO were added to the solutions, then they were stirred during 24 h at room temperature $((25 \pm 2)$ °C). The samples were filtered through a 0.22 μm hydrophilic PTFE syringe filter. The filtrates were diluted to 1:100 ratio to reach optimal concentrations of Ca(II) as well as to decrease the ionic strength to allow for the measurement of the metal ion. The pH of each solution was set to ~2 with HCl solution to avoid the incidental dissolution of $CO_2$ and the subsequent precipitation of $CaCO_3$.

The total amount of Ca(II) was measured with a Perkin Elmer Optima 7000DV Inductively Coupled Plasma Optical Emission (ICP-OES) spectrometer at the wavelength values of 317.93, 393.37 and 396.85 nm (with 3 replicate measurements).

Additionally, 1 mg/L yttrium(III) was added to the samples and the signal of this internal standard was collected at 371.03 nm.

### 2.6. Quantum chemical computations

The initial structures for the $CaLac^+$ and $CaLacOH^0$ complexes were adjusted assuming all possible coordination modes. Furthermore, the dihedral angles were systematically varied along the freely rotating C–C bonds. The geometry optimizations were performed at the M11 range-separated hybrid *meta*-GGA DFT functional [29] coupled with the def2-TZVP basis set as implemented in the Gaussian09 software package [30].

The calculations were carried out in the implicit framework of solvent molecules by utilizing the CPCM solvation model (where water was considered as the solvent) [31]. To model the first coordination sphere of the metal ion, five explicit water molecules were added to the structures. Thus, the coordination number of $Ca^{2+}$ was 6 or 7 depending on the denticity of $Lac^-$. The stability of each structure was checked with frequency calculations.

Coupled cluster single point energy calculations were performed on all the optimized structures using the domain-based local pair-natural orbital coupled-cluster method including single and double excitations and perturbative correction for connected triples (DLPNO-CCSD(T)) [32–46] coupled with the def2-QZVP basis set as implemented in the ORCA 3.0.3 software package [47–55]. These single point calculations utilized the same solvation model and performed using very tight convergence criteria.

## 3. Results and discussion

### 3.1. Complex formation between $Ca^{2+}$ and $Lac^{-}$ ions in neutral medium

In order to examine the $Ca^{2+}$ complexation of $Lac^{-}$ in neutral medium, Ca-ISE potentiometric titrations were performed at $I = 4.0$ M (NaCl) and $T = (25.0 \pm 0.1)$ °C (Fig. 1) The systematic decrease in $[Ca^{2+}]$ with increasing $[Lac^{-}]_{T,0}$ is a sound evidence for complex formation. The three data sets were fitted simultaneously with the *PSEQUAD* program [56] by minimizing the *F* fitting parameter (*F* is the average difference between the observed and calculated data).

Assuming the formation of the 1:1 complex, $CaLac^{+}$, the corresponding formation constant can be expressed as:

$$K_{1,1} = \frac{[CaLac^{+}]c^{o}}{[Ca^{2+}][Lac^{-}]} \quad (1)$$

where $c^{o}$ is the standard molar concentration, 1 mol dm$^{-3}$. Fitting the experimental data, $\log K_{1,1} \pm 3\,SE$ (*i.e.*, standard error) was found be to be $1.23 \pm 0.04$ with $F = 0.073$ log ($[Ca^{2+}]$/M) units (dashed lines in Fig. 1).

Conversely, *F* can be markedly decreased if the $CaLac_2^0$ species is also taken into account. For this complex, the stability product reads as:

$$\beta_{1,2} = \frac{[CaLac_2{}^{0}]c^{o2}}{[Ca^{2+}][Lac^{-}]^{2}} \quad (2)$$

This model yields $\log K_{1,1} = 0.99 \pm 0.02$ and $\log \beta_{1,2} = 1.42 \pm 0.03$ with $F = 0.011$ (solid lines in Fig. 1). In addition to the significant decrease of in the *F* parameter, these constants are consistent with the literature data: $\log K_{1,1} = 0.90$, $\log \beta_{1,2} = 1.24$ ($I = 1$ M) [20] and $\log K_{1,1} = 0.92$, $\log \beta_{1,2} = 1.62$ ($I = 0.5$ M) [21], respectively. The difference is most likely due to the different ionic strength applied during the measurements.

The concentration distribution diagram (Fig. 2) shows that the formation of the $CaLac^{+}$ and $CaLac_2^0$ complexes reaches 48% and 31%, respectively.

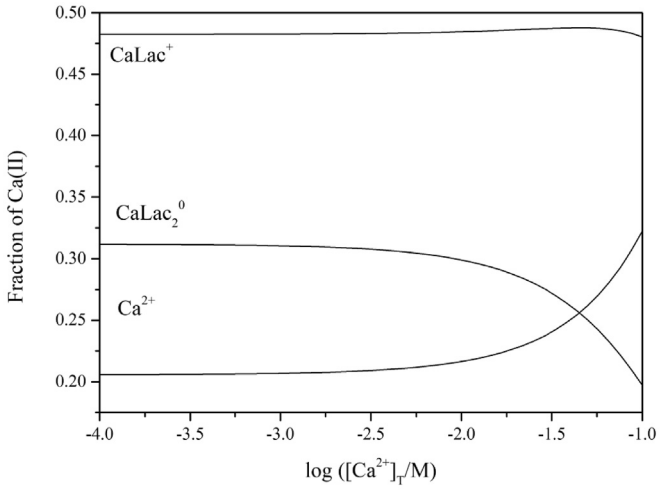


**Fig. 2.** Distribution of Ca(II) among the various aqueous species in a solution containing $[Lac^{-}]_T = 0.24$ M as a function of log ($[Ca^{2+}]_T$/M) using the formation constants of $\log K_{1,1} = 0.99$ and $\log \beta_{1,2} = 1.42$, respectively ($I = 4$ M (NaCl), $T = 25$ °C).

Regarding the formation constant of the 1:1 species, it is very similar to those of D-gluconate ($\log K_{1,1} = 1.08$) and D-heptagluconate ($\log K_{1,1} = 1.00$) [57]. For these two ligands, the binding of the α-hydroxy group was proven by the $^{43}Ca-^{1}H$ long-range couplings that appear in the NMR spectra [58,59]. Consequently, the participation of the OH group in the $Ca^{2+}$ coordination can be postulated for the $CaLac^{+}$ species, too.

The $^{13}C$ NMR shifts of the different carbon nuclei of $Lac^{-}$ are depicted in Fig. 3. It is seen that upon increasing $[Ca^{2+}]_T$, the $^{13}C$ NMR signals shift downfield as a result of complex formation. The measured chemical shifts were fitted as a function of $[Ca^{2+}]_T$ with the aid of the *PSEQUAD* program [56]. Since the proton exchange between $Lac^{-}$ and the various complexes is fast on the $^{13}C$ NMR time scale, the following equation could be used:

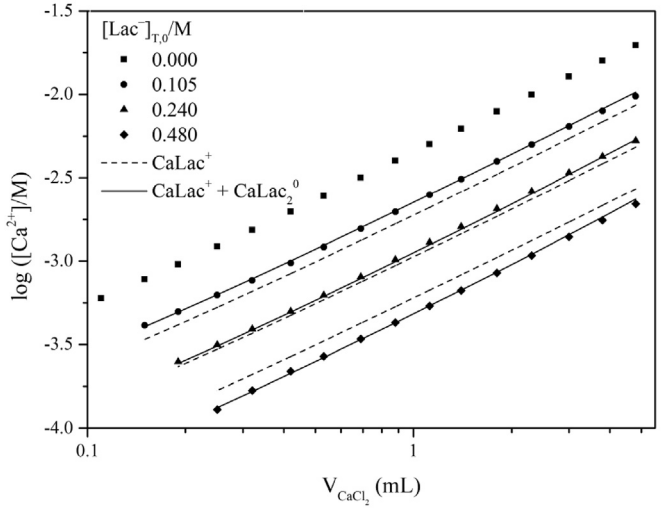


**Fig. 1.** Ca-ISE potentiometric titration curves of solutions containing $Lac^{-}$ and $Ca^{2+}$ in neutral medium as a function of the added titrant volume. Experimental conditions: $I = 4.0$ M (NaCl), $T = (25.0 \pm 0.1)$ °C. Titrand: $V_0 = 45$ mL, $[Ca^{2+}]_{T,0} = 10^{-4}$ M, titrant: $[CaCl_2]_T = 0.2$ M; the initial total concentrations of $Lac^{-}$ are shown in the figure. Symbols: measured data, solid and dashed lines: fitted data assuming different chemical models.

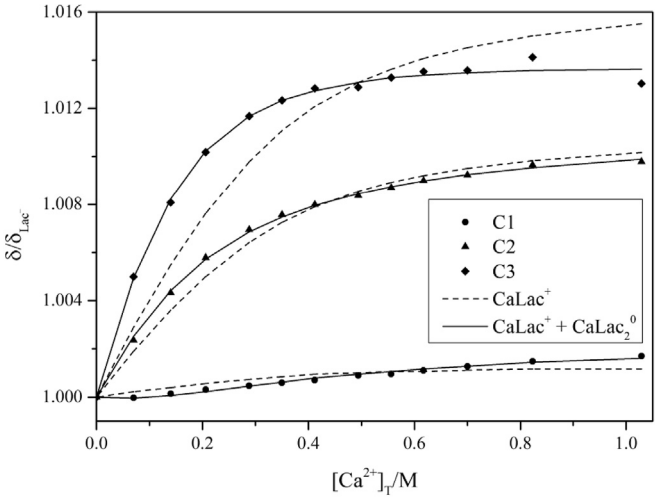


**Fig. 3.** $^{13}C$ NMR chemical shifts of each carbon atom of $Lac^{-}$ as a function of $[Ca^{2+}]_T$. Experimental conditions: $I = 4.0$ M (NaCl), $T = (25 \pm 1)$ °C, $[Lac^{-}]_T = 0.321$ M. Symbols: measured data, solid and dashed lines: fitted data assuming different chemical models. The chemical shifts (δ) were normalized to the chemical shift of the uncomplexed $Lac^{-}$ ion ($\delta_{Lac-}$) for better visualization.

$$\delta_{obs} = \frac{\delta_{Lac^-}[Lac^-] + \delta_{CaLac^+}[CaLac^+] + \delta_{CaLac_2{}^0}\,2\,[CaLac_2{}^0]}{[Lac^-]_T} \quad (3)$$

where $\delta_{obs}$ is the observed chemical shift, $\delta^-_{Lac}$, $\delta^+_{CaLac}$ and $\delta^0_{CaLac2}$ are the limiting chemical shifts of $Lac^-$, $CaLac^+$ and $CaLac^0_2$, respectively.

Since the limiting chemical shifts of the different carbon nuclei of $CaLac^+$ and $CaLac^0_2$ are rather similar, it was not possible to determine both the formation constants and the limiting chemical shifts values independently from these measurements.

However, by treating the formation constants (deduced from Ca-ISE titrations) as non-adjustable parameters, it was possible to calculate the limiting chemical shifts of the complexes. When only the formation of the $CaLac^+$ complex was taken into consideration (with $\log K_{1,1} = 1.23$), the *F* fitting parameter between the measured and the calculated data is relatively large (0.04 ppm, dashed lines in Fig. 3). Expectedly, the inclusion of the $CaLac^0_2$ complex into the model yielded much lower *F* (0.009 ppm, solid lines in Fig. 3), similarly to the results obtained for Ca-ISE potentiometric measurements. The calculated limiting chemical shifts of C1–C3 for the different species are listed in Table 1 (where C1, C2 and C3 belong to the carbon nuclei of the $COO^-$, $CH_2OH$ and $CH_3$ groups, respectively).

In the ESI-MS spectrum of the solution containing $[Lac^-]_T = 0.10$ M and $[Ca^{2+}]_T = 0.05$ M (Fig. 4), the peak corresponding to $CaLac^+$ is expected to appear at 128.9865 *m/z* value. For $CaLac^0_2$, its peak is expected to appear in the spectrum by gaining one positive charge *via* binding a proton, *i. e,.* as $CaLac_2H^+$, at 219.0182 *m/z* value. The formation of both species are confirmed by the presence of these peaks, namely the ones at 128.9733 and 218.9961 *m/z*, respectively. Moreover, further satellites of low intensity can be detected, due to other, low abundance isotopes. The peak positions obtained are in excellent agreement with the calculated ones.

In conclusion, the formation of the $CaLac^0_2$ species is confirmed by two independent methods agreeing well with previous literature results [20,21]. The formation of 1:2 species was also found for other hydroxy carboxylates, such as D-gluconate [21,57], D-heptagluconate and L-gulonate [57].

Regarding the structure of the complexes, the magnitude of the variations of the $^{13}C$ NMR chemical shifts imply that $Ca^{2+}$ is likely to be bound to the $COO^-$ and the OH groups as well. Apart from NMR spectroscopy, the other methods applied in this work cannot provide further information about the binding sites of the complexes formed. To get further insights to the solution structure of the $CaLac^+$ complex, geometry optimizations were carried out with the aid of quantum chemical methods.

For the initial structures, three coordination modes were assumed: (1) monodentate coordination of $COO^-$, (2) bidentate coordination of $COO^-$ and (3) monodentate coordination of both the $COO^-$ and OH groups.

In the most stable isomer of $CaLac^+$ (Fig. 5), the metal ion is bound bidentately to $Lac^-$ according to scenario (3). Interestingly, the binding of the two functions is of similar strength: the Ca–O1A distance is 2.339 Å, while the Ca–O2 one is 2.423 Å. Thus, a strong five-membered chelate ring is formed with the O1A–C1–C2–O2 dihedral angle being −3.355°. This result agrees with the coordination mode proposed from the potentiometric data: similarly to D-gluconate [58] and D-heptagluconate [59], the α-OH group participates in the coordination of $Ca^{2+}$ in addition to $COO^-$.

Furthermore, the $Ca^{2+}$ ion is surrounded by all the five water molecules with the Ca–OW distances ranging from 2.407 to 2.432 Å. Thus, the coordination number of $Ca^{2+}$ is 7 and the coordination geometry is that of a distorted pentagonal bipyramid. Additionally, a hydrogen bond is formed between O1A and O1W (2.077 Å).

The total energy of the second complex is higher by 3.8 kJ mol$^{-1}$. The coordination motif is the same, the difference stems from the somewhat different orientation of water molecules. When both oxygens coordinate $Ca^{2+}$, the energy increases by 8.9 kJ mol$^{-1}$ compared to the global minimum. The highest-energy structures were those in which the $COO^-$ act as a monodentate ligand ($\Delta E = 19.0$ kJ mol$^{-1}$ at least).

**Table 1**
Chemical shifts of the different carbon nuclei of $Lac^-$, $CaLac^+$ and $CaLac^0_2$, calculated from $^{13}C$ NMR measurements. Experimental conditions: $I = 4.0$ M (NaCl), $T = (25 \pm 1)$ °C.

| Species | $\delta_{C1}$ | $\delta_{C2}$ | $\delta_{C3}$ |
|---|---|---|---|
| $Lac^-$ | 182.11 | 67.99 | 20.05 |
| $CaLac^+$ | 182.56 ± 0.03 | 68.75 ± 0.03 | 20.31 ± 0.03 |
| $CaLac^0_2$ | 181.70 ± 0.09 | 68.63 ± 0.09 | 20.56 ± 0.09 |

### 3.2. Acid-base properties of $Lac^-$ in highly alkaline solutions

The deprotonation constant of the alcoholic OH group of $Lac^-$ taking place in highly alkaline medium is defined as

$$K_a = \frac{\left[LacH_{-1}{}^{2-}\right][H^+]}{[Lac^-]c^o}. \quad (4)$$

Upon increasing the concentration of NaOH, the $^{13}C$ NMR signals of $Lac^-$ shift significantly (Fig. 6) indicating deprotonation. The measured δ values were fitted with respect to $[OH^-]_T$ by the *PSEQUAD* program. Since the proton exchange between $LacH^{2-}_{-1}$ and $Lac^-$ is fast on the $^{13}C$ NMR timescale, the following equation could be used:

$$\delta_{obs} = \frac{\delta_{Lac^-}[Lac^-] + \delta_{LacH_{-1}{}^{2-}}\left[LacH_{-1}{}^{2-}\right]}{[Lac^-]_T} \quad (5)$$

where $\delta_{obs}$ is the observed chemical shift, $\delta^-_{Lac}$ and $\delta^{2-}_{LacH-1}$ are the limiting chemical shifts of $Lac^-$ and $LacH^{2-}_{-1}$, respectively. During calculations, the ionic product of water, $pK_w$, was taken as 14.26 [60]. The thus obtained deprotonation constant, $pK_a$, is 15.8 ± 0.2, which is similar to those determined for methanol and ethanol (15.5 and 15.9, respectively [61]). The relatively large uncertainty can be attributed to the low extent of deprotonation, reaching only ~ 10% even at $[OH^-]_T = 4$ M.

### 3.3. Complex formation between $Ca^{2+}$ and $Lac^-$ in highly alkaline medium

Since the acid dissociation constant of the OH group of $Lac^-$ is rather small ($pK_a = 15.8$), $H_2$/Pt potentiometry is unsuitable to examine the complex formation between $Lac^-$ and $Ca^{2+}$ in alkaline medium because of the limited solubility of $Ca(OH)_2$(s). Thus, solubility measurements were chosen to study the Ca(II) complexation of $Lac^-$ in strongly alkaline solutions.

The maximum soluble Ca(II) in solutions containing $[Lac^-]_T = 0.50$ M and $c_{NaOH} = 0.14$–$2.64$ M was measured by ICP-OES. Fig. 7 clearly demonstrates that $[Ca^{2+}]_T$ systematically decreases upon increasing $[OH^-]_T$, which is expected considering the decreasing solubility of portlandite. In the absence of any complexing agents, conversely, log ($[Ca^{2+}]_T$) would be *ca.* −3.5 at $[OH^-]_T = 1$–4 M [62], whilst the present values are significantly higher (*ca.* −2.85 at $[OH^-]_T = 1$ M and −3.1 at $[OH^-]_T = 2.5$ M)

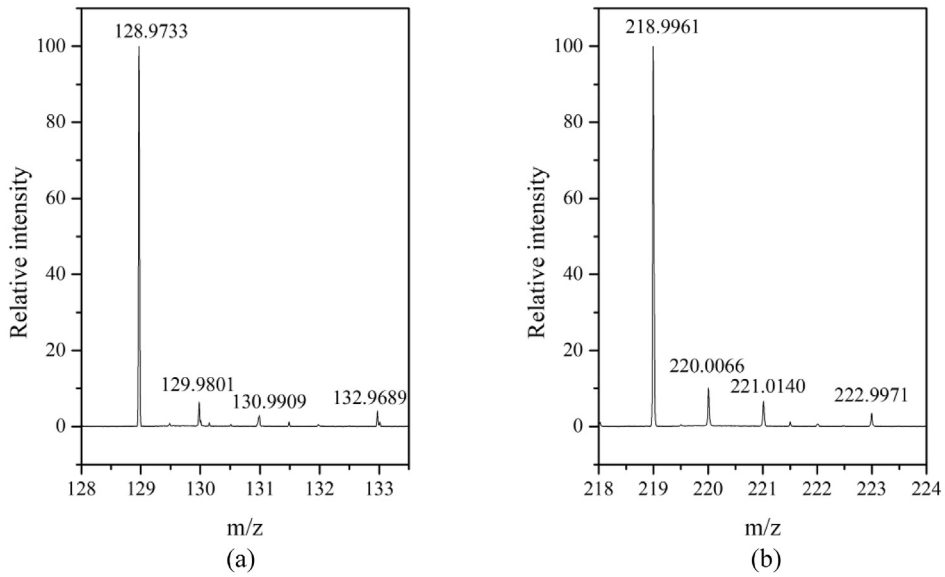


**Fig. 4.** ESI-MS spectra of a solution containing $[Lac^-]_T = 0.10$ M and $[Ca^{2+}]_T = 0.05$ M (positive ion mode), (a): $CaLac^+$, (b): $CaLac_2^0$.

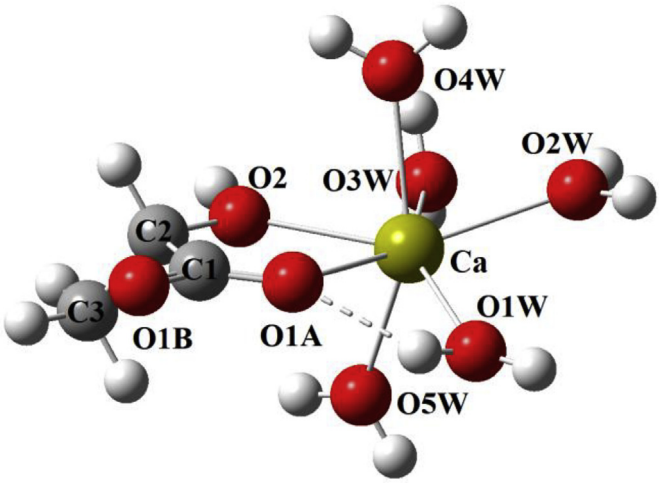


**Fig. 5.** Structure of the $CaLac^+$ complex (global minimum). The geometry optimization was performed at the M11/def2-TZVP level, while the single-point energy calculation was carried out at the DLPNO-CCSD(T)/def2-QZVP level. The solvent effects were taken into account applying the CPCM solvation model. The dashed line indicates the hydrogen bond between O1A and O1W.

corroborating the formation of Ca(II)-Lac-OH mixed complex(es). Such model calculations for the increase in solubility of Ca(II) in the presence and absence of $Lac^-$ is demonstrated in Fig S1.

The measured log ($[Ca^{2+}]_T$/M) values were fitted as a function of $[OH^-]$ with the aid of the *OriginPro* software package [63]. During data evaluation, the formation constants of the following species were held constant (given in brackets): $LacH_{-1}^{2-}$ ($pK_a = 15.6$), $CaLac^+$ (log $K_{1,1} = 0.99$) and $CaLac_2^0$ (log $\beta_{1,2} = 1.42$); $CaOH^+$ (log $K_{1,1} = 0.34$) and $Ca(OH)_2^0$ (log $\beta_{1,2} = 0.88$) [62], as well as $Ca(OH)_{2(s)}$ (log $K_{sp} = -4.52$) [62]. The ionic product of water was taken as $pK_w = 14.26$ [60]. The mathematical relationships applied during data fitting are detailed in the Electronic Supporting Information (ESI). The dotted lines in Fig. 7 show the calculated data if only the $CaLacOH^0$ species is considered with log $\beta_{1,1,1} = 1.7 \pm 0.1$, where $\beta_{1,1,1}$ reads as

$$\beta_{1,1,1} = \frac{[CaLacOH^0]c^{o2}}{[Ca^{2+}][Lac^-][OH^-]} \quad (6)$$

The systematic and significant deviations between the observed and calculated data ($F = 0.078$), however, suggest the formation of at least one more species. By including the formation of the $CaLac(OH)_2^-$ species, the $F$ fitting parameter could be lowered to 0.012 (solid line in Fig. 7). The corresponding formation constants are log $\beta_{1,1,1} = 1.35 \pm 0.09$ and log $\beta_{1,1,2} = 1.43 \pm 0.06$, where $\beta_{1,1,2}$ is

$$\beta_{1,1,2} = \frac{[CaLac(OH)_2^-]c^{o3}}{[Ca^{2+}][Lac^-][OH^-]^2} \quad (7)$$

When only the formation of this 1:1:2 species is considered, $F$ increases to 0.053 (dashed line in Fig. 7) pointing to the simultaneous formation of these two complexes.

It is worth discussing that the log $\beta_{1,1,1}$ and log $\beta_{1,1,2}$ constants are practically the same considering their error intervals. It has to be noted that dividing eq. (6) by eq. (7) leads to the

$$\frac{[CaLac(OH)_2^-]}{[CaLacOH^0]} = [OH^-]\frac{\beta_2}{\beta_1} \quad (8)$$

equation. Since $\beta_2/\beta_1 = 1.2$, this equation clearly shows that none of these species can be omitted at around $[OH^-]_T \sim 1$ M. This is in complete agreement with Fig. 7.

By the distribution diagram presented in Fig. 8, both of these species form in significant quantities. It is seen that above $[OH^-]_T = 1$ M, the $CaLac(OH)_2^-$ complex becomes predominant. It is also shown in Fig. 8 that under the same experimental conditions (*i.e.*, $[OH^-]_T = 0.2$–$2.6$ M) but in the absence of $Lac^-$, calcium is present almost exclusively as $CaOH^+$ and $Ca(OH)_2^0$. Consequently, both $CaLacOH^0$ and $CaLac(OH)_2^-$ most probably contain a $Lac^-$ ligand coordinated to a $CaOH^+$ or a $Ca(OH)_2^0$ unit. Furthermore, if the ligand in these species was $LacH_{-1}^{2-}$ (*i.e.*, the hydroxy group of lactate was deprotonated), the formation constants would be expected to be significantly larger, as the alcoholate moiety is a significantly stronger base, therefore stronger complexant, than the hydroxy group. For instance, for D-gluconate, log $\beta_{1,1,1}$ was found to

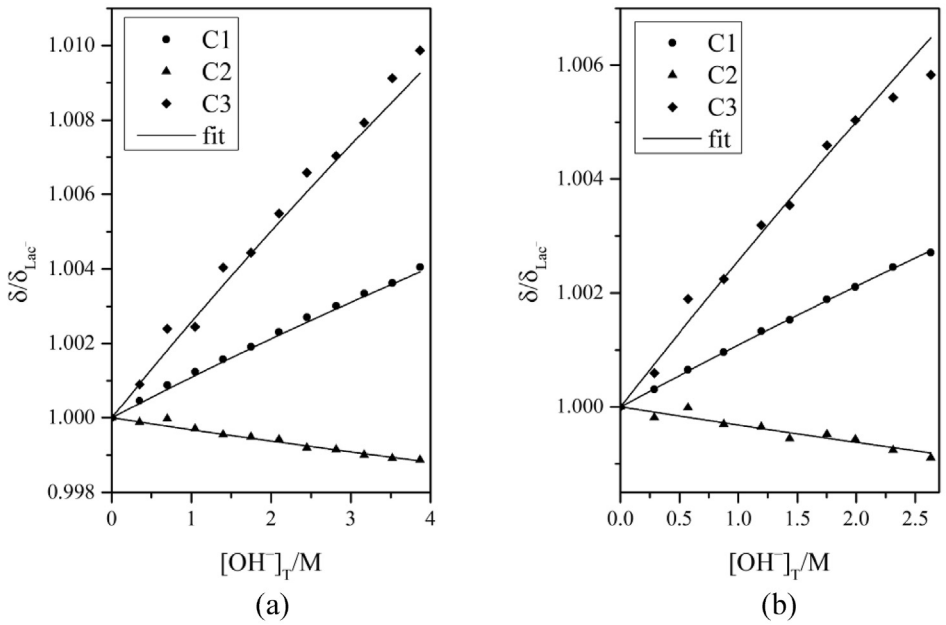


**Fig. 6.** $^{13}C$ NMR chemical shifts of each carbon atom of $Lac^-$ in terms of $[OH^-]_T$. Experimental conditions: $I = 4.0$ M (NaCl), $T = (25 \pm 1)$ °C, $[Lac^-]_T = 0.0960$ M (a) and 0.1525 M (b). Symbols: measured data, solid lines: fitted data assuming the one-fold deprotonation of $Lac^-$. The measured δ values were normalized to those of the neat $Lac^-$ ion for better visualization.

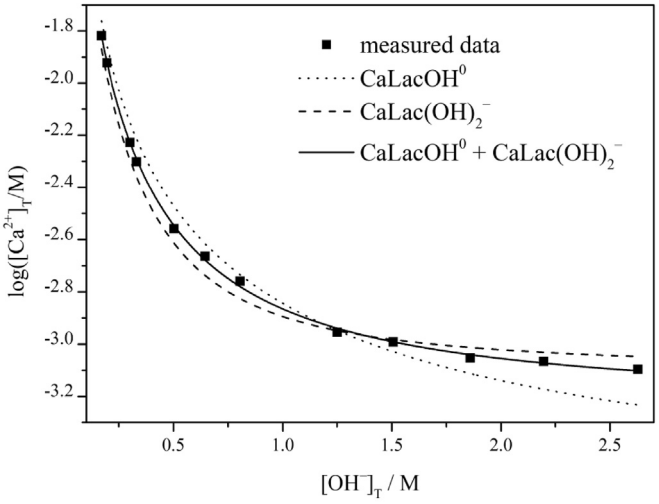


**Fig. 7.** Measured and calculated $\log([Ca^{2+}]_T/M)$ values as a function of $[OH^-]_T$. Experimental conditions: $I = 4.0$ M (NaCl), $T = (25 \pm 2)$°C, $[Lac^-]_T = 0.50$ M, $[OH^-]_T = 0.17–2.63$ M. Dotted, dashed and solid lines represent the fitted data by assuming the formation of only the $CaLacOH^0$ complex, only the $CaLacOH^-$ complex or both species.

be 2.53 [60] as a token of ligand deprotonation.

The structure of the $CaLacOH^0$ complex was also studied *via* quantum chemical computations. The three coordination motifs applied for the $CaLac^+$ species were also used for the initial structures of the 1:1:1 complex. For each linkage isomer, further isomers were constructed by deprotonating the water molecules one by one as well as by assuming the deprotonation of the OH group.

It was found that the sevenfold coordination of $Ca^{2+}$ was not preferred in the most stable structures. That is, if the $COO^-$ coordinated in a bidentate manner, it became monodentate or one water was pulled away from the coordination sphere of $Ca^{2+}$ during structure optimization. The same phenomenon occurred if both the $COO^-$ and the OH groups acted as binding sites. As a result, the sixfold coordination of the metal ion is more favourable in the deprotonated complexes.

The lowest-energy structure is depicted in Fig. 9. The $COO^-$ acts as a monodentate binding site leading to distorted octahedral geometry around $Ca^{2+}$. Here, an equatorial water molecule which is disposed *trans* to the O1A nucleus undergoes deprotonation and the O1A–Ca–OH bond angle is 153.7°. The Ca–O1A bond length is 2.494 Å, being considerably higher compared to the $CaLac^+$ complex (2.339 Å). In conclusion, the interaction between $Ca^{2+}$ and the $COO^-$ moiety is significantly weakened by the Ca–OH bond which is, in turn, much stronger (2.235 Å) than the one in the $CaLac^+$ species (2.423 Å).

This structure has a complex network of hydrogen bonds established between the 4 W water molecule and the $OH^-$ ion (1.647 Å), the 1 W water and O1A (2.288 Å), the O2W as well as the O3W water molecules and O1B (2.204 Å and 2.221 Å). Additionally, an internal hydrogen bond is formed between the OH group of $Lac^-$ and the O1B nucleus (1.965 Å). The Ca–water distances were found to be 2.408–2.497 Å.

The next structure has the total energy higher by only 0.5 kJ $mol^{-1}$. The metal ion is coordinated in a bidentate manner by $COO^-$, whilst one water molecule seems to be outside the first coordination sphere (2.568 Å).

Having the OH group of $Lac^-$ deprotonated, the structures become less favourable: the energy of the most stable complex with an alcoholate moiety is higher by 7.0 kJ $mol^{-1}$ compared to the global minimum. (Generally, it was found that the alcoholate group abstracts a proton from a neighbouring solvent molecule during the optimization procedure.)

In conclusion, during the course of the formation of the $CaLacOH^0$ species, the deprotonation occurs on a coordinated water molecule more likely than the OH group of the ligand. This favourable ionization of the $H_2O$ molecules is supported by the formation constant deduced from solubility measurements as well as by the present quantum chemical computations.

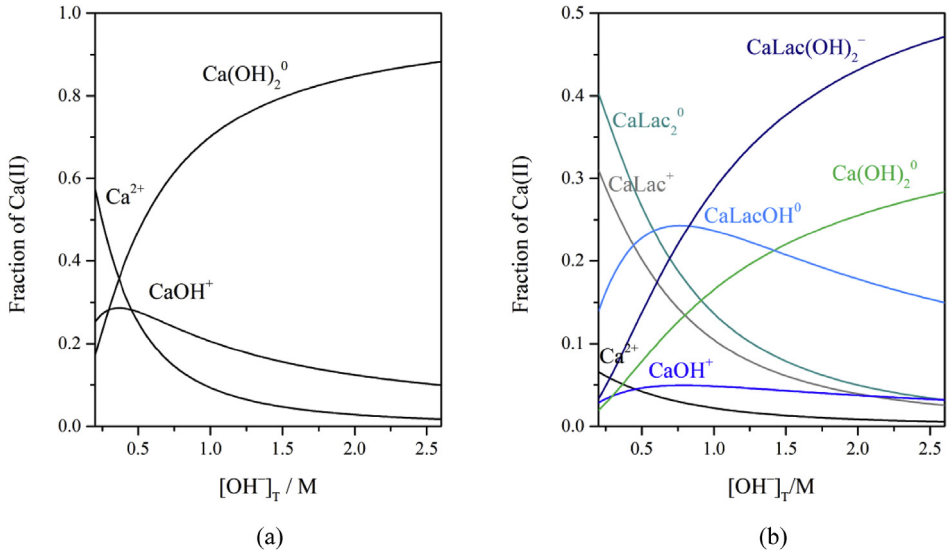


**Fig. 8.** Distribution of Ca(II) among the various aqueous species in the absence of $Lac^-$ (a) and in the presence of $[Lac^-]_T = 0.50$ M (b) as a function of $[OH^-]$ assuming heterogeneous equilibrium with respect to $Ca(OH)_2(s)$ ($I = 4$ M (NaCl), $T = 25$ °C).

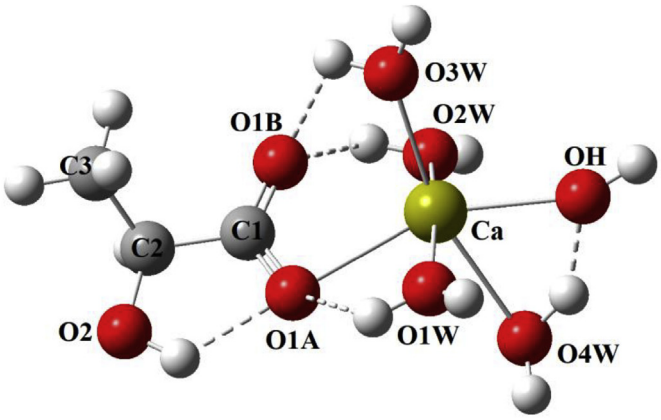


**Fig. 9.** Structure of the $CaLacOH^0$ complex (global minimum). The geometry optimization was performed at the M11/def2-TZVP level, while the single-point energy calculation was carried out at the DLPNO-CCSD(T)/def2-QZVP level. The solvent effects were taken into account applying the CPCM solvation model. The dashed lines indicate the hydrogen bonds.

## 4. Conclusions

From Ca-ISE potentiometric measurements conducted in neutral medium, $Lac^-$ was found to form weak complexes with calcium with 1:1 and 1:2 composition (*i.e.*, $CaLac^+$ and $CaLac_2^0$). The formation of these complexes was confirmed by $^{13}C$ NMR spectroscopy and ESI-MS measurements. The structure of the $CaLac^+$ complex was optimized by molecular modelling calculations, and $Lac^-$ was found to coordinate the $Ca^{2+}$ ion bidentately, through one carboxylate oxygen and the hydroxy group. The coordination number around the metal ion was calculated to be seven.

The alkaline deprotonation of the alcoholic OH group of $Lac^-$ has been investigated by $^{13}C$ NMR spectroscopy. $Lac^-$ was found to be a very weak acid, its proton dissociation constant was determined to be $pK_a = 15.8 \pm 0.2$, which is somewhere between that of methanol and ethanol.

The complex formation between $Ca^{2+}$ and $Lac^-$ in alkaline medium was studied by solubility experiments and the formation of the $CaLacOH^0$ and $CaLac(OH)_2^-$ species was deduced. Since the formation constant of these species is lower than that of complexes in which the ligand contains an alcoholate moiety, furthermore, under the experimental conditions applied, calcium is almost exclusively present as $CaOH^+$ and $Ca(OH)_2^0$ aqueous species, it is suggested that in these complexes the water molecule(s) coordinated to the $Ca^{2+}$ ion deprotonate(s). This is supported by the geometry optimization of the $CaLacOH^0$ complex, *i.e.,* the lowest energy structure was found to involve a $Lac^-$ coordinating to the $Ca^{2+}$ ion by the carboxylate group in a monodentate manner, while one water molecule coordinated to the metal ion was found to be deprotonated.

## Acknowledgements

This work was supported by the NKFIH K 124 265 and the UNKP-17-2 grants. All these supports are highly appreciated.

## Appendix A. Supplementary data

Supplementary data to this article can be found online at https://doi.org/10.1016/j.molstruc.2018.12.020.

## References

[1] G. Baston, J. Berry, K. Bond, K. Boult, M. Brownsword, C. Linklater, J. Alloy. Comp. 213 (1994) 475–480.
[2] K. Vercammen, M.A. Glaus, L.R. Van Loon, Radiochim. Acta 89 (2001) 393–401.
[3] J. Tits, E. Wieland, M.H. Bradbury, Appl. Geochem. 20 (2005) 2082–2096.
[4] X. Gaona, V. Montoya, E. Colas, M. Grive, L. Duro, J. Contam. Hydrol. 102 (2008) 217–227.
[5] M.J. Keith-Roach, Sci. Total Environ. 396 (2008) 1–11.
[6] M.A. Glaus, L.R. van Loon, S. Achatz, A. Chodura, K. Fischer, Anal. Chim. Acta 398 (1999) 111–122.
[7] M.A. Glaus, L.R. van Loon, Environ. Sci. Technol. 42 (2008) 2906–2911.
[8] C.J. Knill, J.F. Kennedy, Carbohydr. Polym. 51 (2003) 281–300.
[9] L.R. Van Loon, M.A. Glaus, S. Stallone, A. Laube, Environ. Sci. Technol. 31 (1997) 1243–1245.
[10] M. Almond, D. Belton, P.N. Humphreys, A.P. Laws, Carbohydr. Res. 427 (2016) 48–54.
[11] I. Pavasars, J. Hagberg, H. Borén, B. Allard, J. Polym. Environ. 11 (2003) 39–47.
[12] G. Richards, H. Sephton, J. Am. Chem. Soc. (1957) 4492–4499.
[13] R. Portanova, L.H.J. Lajunen, M. Tolazzi, J. Piispanen, Pure Appl. Chem. 75 (2003) 495–540.
[14] S. Glab, M. Maj-Zurawska, P. Lukomski, A. Hulanicki, Anal. Chim. Acta 273 (1993) 493–497.
[15] R. Gosh, V.S.K. Nair, J. Inorg. Nucl. Chem. 32 (1970) 3025–3032.

[16] J. Piispanen, L.H.J. Lajunen, Acta Chem. Scand. 49 (1995) 235–240.
[17] R.K. Cannan, A. Kibrick, J. Am. Chem. Soc. 60 (1938) 2314–2320.
[18] J. Schubert, A. Lindenbaum, J. Am. Chem. Soc. 74 (1952) 3529–3532.
[19] M. Vavrusova, M.B. Munk, L.H. Skibsted, J. Agric. Food Chem. 61 (2013) 8207–8214.
[20] F. Verbeek, H. Thun, Anal. Chim. Acta 33 (1965) 378–383.
[21] M. Masone, M. Vicedomini, Ann. Chim. Rome 71 (1981) 517.
[22] A. Kondoh, T. Oi, Z. Naturforsch Sect. A J. Phys. Sci. 52a (1997) 351–357.
[23] H. Deelstra, F. Verbeek, Anal. Chim. Acta 31 (1964) 251–257.
[24] L.E. Roy, L.R. Martin, Dalton Trans. 45 (2016) 15517–15522.
[25] A. Barkleit, J. Kretzschmar, S. Tsushima, M. Acker, Dalton Trans. 43 (2014) 11221–11232.
[26] G. Tian, L.R. Martin, L. Rao, Inorg. Chem. 49 (2010) 10598–10605.
[27] P. Sipos, G. Hefter, P. May, Analyst 125 (2000) 955–958.
[28] G. Peintler, Spline Calculus, University of Szeged, Szeged, Hungary, 2008, Version 2.12a.
[29] R. Peverati, D.G. Truhlar, J. Phys. Chem. Lett. 2 (2011) 2810–2817.
[30] Gaussian09, Revision E.01, Gaussian, Inc., Wallingford, CT, U.S., 2013.
[31] M. Cossi, N. Rega, G. Scalmani, V. Barone, J. Comput. Chem. 24 (2003) 669–681.
[32] C. Riplinger, B. Sandhoefer, A. Hansen, F. Neese, J. Chem. Phys. 139 (2013) 134101–134113.
[33] W.B. Schneider, G. Bistoni, M. Sparta, M. Saitow, C. Riplinger, A.A. Auer, F. Neese, J. Chem. Theor. Comput. 12 (2016) 4778–4792.
[34] C. Riplinger, P. Pinski, U. Becker, E.F. Valeev, F. Neese, J. Chem. Phys. 144 (2016) 24109–24118.
[35] F. Pavosevic, P. Pinski, C. Riplinger, F. Neese, E.F. Valeev, J. Chem. Phys. 144 (2016) 144109–144121.
[36] A. Kubas, D. Berger, H. Oberhofer, D. Maganas, K. Reuter, F. Neese, J. Phys. Chem. Lett. 7 (2016) 4207–4212.
[37] M. Isegawa, F. Neese, D.A. Pantazis, J. Chem. Theor. Comput. 12 (2016) 2272–2284.
[38] Y. Guo, K. Sivalingam, E.F. Valeev, F. Neese, J. Chem. Phys. 144 (2016) 94111–94126.
[39] A.K. Dutta, F. Neese, R. Izsak, J. Chem. Phys. 145 (2016) 34102–34109.
[40] D. Datta, S. Kossmann, F. Neese, J. Chem. Phys. 145 (2016) 114101–114118.
[41] P. Pinski, C. Riplinger, E.F. Valeev, F. Neese, J. Chem. Phys. 143 (2016) 34108.
[42] B. Mondal, F. Neese, S.F. Ye, Inorg. Chem. 54 (2015) 7192–7198.
[43] D.G. Liakos, M. Sparta, M.K. Kesharwani, J.M.L. Martin, F. Neese, J. Chem. Theor. Comput. 11 (2015) 1525–1539.
[44] D.G. Liakos, F. Neese, J. Chem. Theor. Comput. 11 (2015) 2137–2143.
[45] D.G. Liakos, F. Neese, J. Chem. Theor. Comput. 11 (2015) 4054–4063.
[46] O. Demel, J. Pittner, F. Neese, J. Chem. Theor. Comput. 11 (2015) 3104–3114.
[47] F. Neese, Wiley Interdiscip. Rev. Comput. Mol. Sci. 2 (2012) 73–78.
[48] R. Izsak, F. Neese, Mol. Phys. 111 (2013) 1190–1195.
[49] R. Izsak, F. Neese, J. Chem. Phys. 135 (2011) 144105–144115.
[50] S. Kossmann, F. Neese, J. Chem. Theor. Comput. 6 (2010) 2325–2338.
[51] S. Kossmann, F. Neese, Chem. Phys. Lett. 481 (2009) 240–243.
[52] F. Neese, F. Wennmohs, A. Hansen, U. Becker, Chem. Phys. 356 (2009) 98–109.
[53] F. Neese, J. Comput. Chem. 24 (2003) 1740–1747.
[54] A.K. Dutta, F. Neese, R. Izsak, J. Chem. Phys. 144 (2016) 34102–34109.
[55] G.J. Christian, F. Neese, S.F. Ye, Inorg. Chem. 55 (2016) 3853–3864.
[56] L. Zékány, I. Nagypál, G. Peintler, PSEQUAD for Chemical Equilibria, Update 5–5.10, Hungary, 2000–2008.
[57] B. Kutus, D. Ozsvár, N. Varga, I. Pálinkó, P. Sipos, Dalton Trans. 46 (2017) 1065–1074.
[58] A. Pallagi, P. Sebők, P. Forgó, T. Jakusch, I. Pálinkó, P. Sipos, Carbohydr. Res. 345 (2010) 1856–1864.
[59] A. Pallagi, Z. Csendes, B. Kutus, E. Czeglédi, G. Peintler, P. Forgo, I. Pálinkó, P. Sipos, Dalton Trans. 42 (2013) 8460–8467.
[60] Á. Buckó, B. Kutus, G. Peintler, I. Pálinkó, P. Sipos, Polyhedron 158 (2019) 117–124, https://doi.org/10.1016/j.poly.2018.10.034.
[61] P. Ballinger, F.A. Long, J. Am. Chem. Soc. 82 (1960) 795–798.
[62] B. Kutus, A. Gácsi, A. Pallagi, I. Pálinkó, G. Peintler, P. Sipos, RSC Adv. 6 (2016) 45231–45240.
[63] OriginPro, OriginLab, Northhampton, MA, U.S., 2011, Version 8.6.